RSC Advances

PAPER

View Article Online
View Journal | View Issue

Cite this: *RSC Adv.*, 2014, **4**, 19370

Spectral properties of 4-(4-hydroxy-1-naphthylazo)benzenesulfonic acid and its application for colorimetric determination of trace Fe^{3+}

Lei Hu, Li Nie, Guangnian Xu, Han Shi, Xiaoqing Xu, Xiangzhong Zhang and Zhengquan Yan*

Received 24th January 2014
Accepted 6th March 2014

DOI: 10.1039/c4ra00512k

www.rsc.org/advances

A multifunctional dye, 4-(4-hydroxy-1-naphthylazo)benzenesulfonic acid (**HNABA**) was identified and synthesized. The dye, combining hydroxyl, azo and carboxyl groups, possessed excellent optical absorption properties changing with pH, solvent and coexisting metal ions. In particular, its spectral properties remained extremely stable under acid or neutral conditions and it was effectively applied for colorimetric determination of Fe^{3+} from brick-red to light red in aqueous solution under physiological pH conditions (pH 7.0). Under the optimum conditions, the detection possessed a linear range of 9.5–400 $\times$ 10^{-8} mol L^{-1} with a correlation coefficient (R) of 0.9938 and a limit detection (3σ, n = 20) of 4.2 $\times$ 10^{-9} mol L^{-1}. The relative standard deviation (R.S.D.) was lower than 3.5% (n = 5). The proposed method was successfully used to determine trace Fe^{3+} in three real environmental water samples. The mechanism of action between **HNABA** and Fe^{3+} ion is discussed in detail.

1. Introduction

Detection of metal ions has continued to attract tremendous attention in recent years due to its importance in environmental, biology and chemistry domains. Iron, the third most abundant element in the earth's crust, is not only a very important macro-element in the environment, but also an essential mineral nutrient for human health.[1,2] People who lack iron will suffer from iron deficiency anemia and other serious effects on human health, while excess iron would cause an increased risk of cancer, heart disease and other illnesses such as haemochromatosis.[3–8] Therefore, there is an urgent need to develop chemical sensors that are capable of detecting and monitoring iron levels in environmental samples. Considerable efforts have been made to develop various detection methods, such as fluorescent spectrometry,[9–14] electro-chromic techniques[15,16] flow injection spectro-photometry,[17,18] chromatography,[19,20] mass spectrometry,[21] nuclear magnetic resonance,[22] and inductively coupled plasma mass spectrometry.[23] However, these instrumentally intensive methods often require utilizing sophisticated instrumentation or complicated pretreatment procedures, and are not suitable for on-line or in-field monitoring. By virtue of its simplicity, rapidity, non-destructive characteristics and especially the fact that the naked eye, rather than complex instruments,[24–29] can be used to observe change, colorimetric sensors for Fe^{3+} have attracted considerable attention in recent years.[30–33] Typically, Yun *et al.*[31] presented an easy naked-eye detection method for Fe^{3+} with a detection limit of 0.024 μg mL^{-1}, based on 1-nitroso-2-naphthol, an excellent color-forming chelating agent. Adebayo *et al.*[34] found a novel 8-hydroxyquinoline-based colorimetric sensor for the simple and rapid determination of Fe^{3+} using the reaction of Fe^{3+} with the sensor to form a metaloxine complex in chloroform solution. Wallace *et al.*[30] developed a system that was able to detect low levels of Fe^{3+} using a squaraine dye to model on siderophores. All these confirm that organic colorimetric sensors are a promising, easy and practical strategy for detecting Fe^{3+}. However, the sensitivity of common colorimetric sensors is still lower than that of the instrumentally intensive methods mentioned above. To develop novel and efficient colorimetric sensing materials will remain a big challenge for a long time in the future.

Herein, to improve the sensitivity and selectivity of Fe^{3+} detection in aqueous systems, a multifunctional dye, 4-(4-hydroxy-1-naphthylazo)benzenesulfonic acid (**HNABA**), was identified and applied for Fe^{3+} detection after its optical properties were studied in detail. The multifunctional dye was expected to possess high selectivity and sensitivity to Fe^{3+} using both a hydroxyquinoline group[31] and an –N=N– group[35,36] as chelating groups and to further increase the solubility in aqueous solution combining $-SO_3H$, –OH and –N=N– groups.

Anhui Provincial Laboratory of Biomimetic Sensor and Detecting Technology & Solar Photovoltaic Materials Research Center, West Anhui University, Lu'an 237012, China. E-mail: yanzhq2008@163.com; Tel: +86 5643305801

The action mechanism between **HNABSC** and Fe^{3+} was discussed by means of Job's plots and theoretical calculation.

2. Experiments

2.1 Reagents and apparatus

All the chemicals in the experiment were of AR grade and used as received from Sinopharm Chemical Reagent Co. Ltd. Water used throughout was doubly deionized.

A 1.0 mmol L^{-1} Fe^{3+} standard solution for testing was prepared in doubly deionized water at room temperature and diluted to the appropriate concentration daily. **HNABA** was synthesized according to our previous work[37,38] and a 5.0×10^{-3} mol L^{-1} **HNABA** stock solution was prepared in doubly deionized water at room temperature and stored at 4 °C. Phosphate buffers (PB) were prepared by mixing a 0.01 mol L^{-1} H_3PO_4 solution, a 0.01 mol L^{-1} K_2HPO_4 solution, a 0.01 mol L^{-1} KH_2PO_4 solution or a 0.01 mol L^{-1} KOH solution in the proper ratio to achieve the desired pH (pH = 3.0, 4.0, 5.0, 6.0, 7.0, 7.5, 8.0, 9.0, 10.0).

FTIR spectra of **HNABA** using a KBr disc were acquired using a Nicolet NEXUS 870 FTIR spectrophotometer at room temperature from 4000–500 cm^{-1}. ^1H NMR spectra were recorded using a Bruker AMX-500 spectrometer operating at 400 MHz, with tetramethyl-silane (TMS) used as the reference and D_2O as solvent. Elemental analysis was conducted using an Elemental Vario EL-III apparatus. UV-vis spectra were recorded on a Lambda 35 UV/vis spectrometer using a 1 cm square quartz cell. pH was measured by a PHS-25 pH meter.

2.2 Preparations of HNABA

According to the literature,[37,38] *p*-amino benzenesulfonic acid (0.87 g, 5 mmol) was dissolved in an ice–water solution of 15% sodium nitrite (0.38 g, 5.5 mmol). After cooling to 0 °C, the solution was added to concentrated hydrochloric acid (1.2 mL) and stirred for 30 min. The excess nitrous acid was destroyed with about 5 mg urea. The mixture was then added dropwise to 10 mL buffered aqueous solution (KH_2PO_4/Na_2HPO_4, pH = 6) containing naphthol (0.73 g, 5 mmol) and stirred for another 2 h at 0–5 °C. The resultant precipitate was filtered and purified by recrystallizing three times from ethanol to provide dark red crystals of **HNABA** in a yield of 92.1%.

IR (KBr), ν (cm^{-1}): 3433–2500 (OH, SO_3H), 1594, 1518 (Ar), 1376 (Ar–N (R_1R)), 1169 (S–O). ^1H-NMR (D_2O, 400 Hz) δ (ppm): 8.74 (d, $J = 8.5$ Hz, 1H, Ar–H), 8.61 (d, $J = 8.4$ Hz, 1H, Ar–H), 8.40 (d, $J = 8.4$ Hz, 1H, Ar–H), 8.12 (d, $J = 7.8$ Hz, 1H, Ar–H), 8.06 (d, $J = 7.8$ Hz, 1H, Ar–H), 7.48 (t, $J = 6.4$ Hz, 1H, Ar–H), 7.51 (t, $J = 6.7$ Hz, 1H, Ar–H), 7.15 (t, $J = 6.5$ Hz, 1H, Ar–H), 5.15 (s, 1H, –OH). Anal. calcd for $C_{16}H_{12}N_2SO_4$: H, 3.68; C, 58.53; N, 8.51; S, 9.77%. Found: H, 3.73; C, 58.49; N, 8.50; S, 9.79%.

2.3 Fe^{3+} detection procedure

For the Fe^{3+} determination, 1.0 mL PB (pH 7.0), 1.0 mL 5.0×10^{-4} mol L^{-1} of **HNABA** and 1.0 mL of the appropriate Fe^{3+} solution or sample were transferred into a 10 mL volumetric flask. The mixture was stirred thoroughly and finally diluted to 10 mL with doubly deionized water. After 20 min, the absorption spectra were measured from 200 nm to 600 nm and the band-slit was set as 2.0 nm. The absorption intensity difference at 478 nm was used for quantitative analysis. The decreased absorption intensity of **HNABA** was represented as $\Delta A = A_0 - A$, where A_0 and A were the absorption intensities of the systems in the absence and presence of Fe^{3+}, respectively.

3. Results and discussion

3.1 The UV-vis absorption spectrum of HNABA

It is well known that **HNABA** is a strong polar compound, whose solubility is quite low in nonpolar solvents. To illustrate the effect of solvents on the absorption spectrum of **HNABA**, the UV-vis spectra in different polar solvents, *i.e.*, *N*,*N*-dimethyl formamide (DMF), tetrahydrofuran (THF), acetone, ethanol and water were recorded as shown in Fig. 1.

In Fig. 1, we can find that **HNABA** has a strong and sharp absorption peak at *ca.* 478 nm in polar protic water and ethanol, attributed to the whole molecular π-conjugated system, with molar absorptivity (ε) of 2.54×10^4 L mol^{-1} cm^{-1} and 1.95×10^4 L mol^{-1} cm^{-1}, respectively, meaning that **HNABA** exists in the form of a monomolecule, *i.e.*, polar protic water and ethanol are both good solvents for **HNABA**. However in polar aprotic acetone, THF and DMF, the absorption intensity at *ca.* 478 nm decreases and a new blue-shifted absorption peak emerges at *ca.* 420 nm. The widening and blue-shift of the absorption might be attributed to the H-aggregation of **HNABA** in poor solvents such as acetone, THF and DMF.[39,40] The conclusion could be further confirmed by the fact that the absorptions at *ca.* 240, 266, 290, 330 nm appear clearly in polar protic water and ethanol while they decrease or disappear almost in polar aprotic acetone, THF and DMF, attributed to the $\pi \rightarrow \pi^*$, $n \rightarrow \pi^*$ transitions of the C=C, N=N and O=C bonds in the non-conjugated benzenesulfonic acid and naphthol moieties.

For an acidic **HNABA** molecule, the pH of the system will have a more significant influence on the form in which it exists and so will make its absorption spectrum change. Here the effect of pH on the absorption spectrum was investigated in polar protic water with a pH range of 3.0–10.0. As shown in

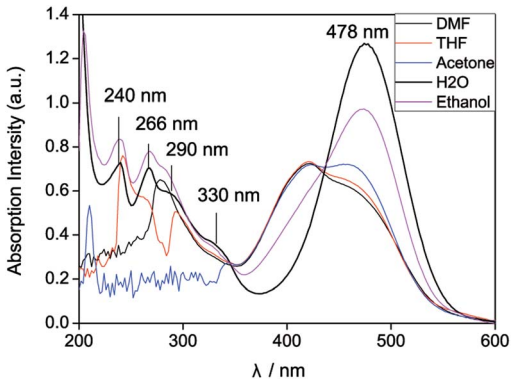

Fig. 1 The UV-vis spectra of **HNABA** in polar solvents, DMF, THF, acetone, water and ethanol.

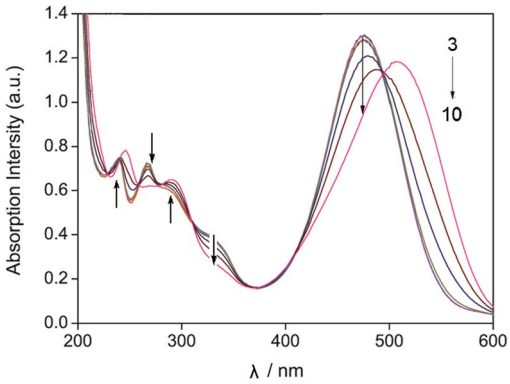

Fig. 2 Effect of pH on the UV-vis spectra of **HNABA** (From up to down: 3.0, 4.0, 5.0, 6.0, 7.0, 7.5, 8.0, 9.0, 10.0).

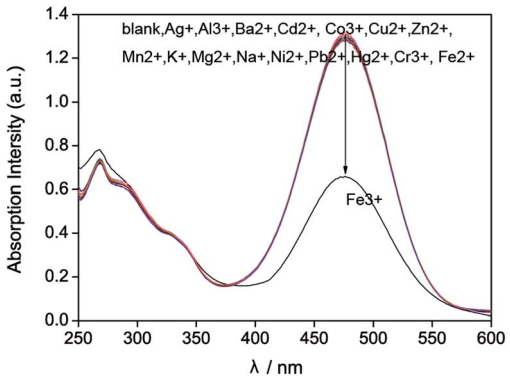

Fig. 3 Effect of different metal ions on the UV-vis spectra of **HNABA**.

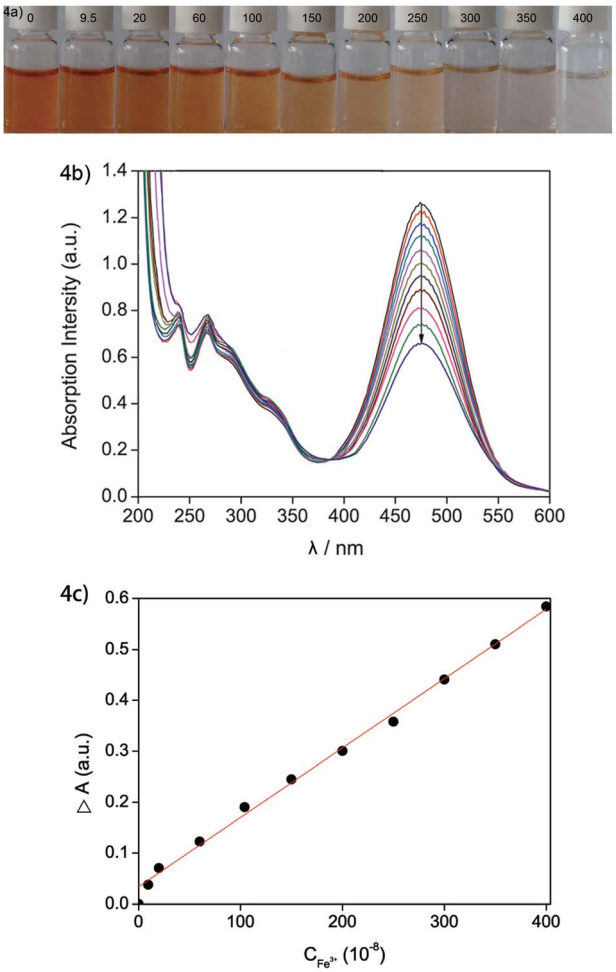

Fig. 4 The colour change (4a) and the absorption spectra (4b) of **HNABA** in different Fe^{3+} concentrations (from up to down: 0, 9.5, 20, 60, 100, 150, 200, 250, 300, 350, 400 × 10^{-8} mol L^{-1}); and the linear relationship between the Δ*A* of **HNABA** at 478 nm and $c_{Fe^{3+}}$ (4c).

Fig. 2, it is interesting to find that the absorption at 478 nm keeps quite stable as long as the pH is less than 7.0. When pH is more than 8.0, the absorption intensity at 478 nm decreases gradually and red shifts. The reason may be that the SO_3H and OH groups in **HNABA** molecules are all ionized to SO_3^- and O^- ions under basic conditions, which would enlarge the whole molecular π-conjugated system, but decrease the molecular dipole moment. The same phenomenon is also found in the absorbance at *ca.* 240, 266, 290, 330 nm as shown in Fig. 2, meaning that **HNABA** could possess good optical absorption properties under a wide pH range, *i.e.*, physiological conditions (pH *ca.* 7.0) will be selected in the next experiments.

3.2 Special response to Fe^{3+}

To demonstrate the selectivity of **HNABA** sensing for Fe^{3+}, we investigated its colorimetric response to some other environmentally relevant metal ions, *i.e.*, Ag^+, Al^{3+}, Ba^{2+}, Cd^{2+}, Co^{3+}, Cu^{2+}, Zn^{2+}, Mn^{2+}, K^+, Mg^{2+}, Na^+, Ni^{2+}, Pb^{2+}, Hg^{2+}, Cr^{3+} and Fe^{2+} at high concentrations in aqueous solutions at pH 7.0. After the addition of 100 equiv. (4.0×10^{-4} mol L^{-1}) of the different metal ions above and Fe^{3+} (4.0×10^{-6} mol L^{-1}), the relative changes in absorption intensities of the sensing system were recorded as shown in Fig. 3, respectively. It can be seen from Fig. 3 that the absorption intensities of the **HNABA** sensing system in the presence of Ag^+, Al^{3+}, Ba^{2+}, Cd^{2+}, Co^{3+}, Cu^{2+}, Zn^{2+}, Mn^{2+}, K^+, Mg^{2+}, Na^+, Ni^{2+}, Pb^{2+}, Hg^{2+}, Cr^{3+} and Fe^{2+} show negligible change even with 100-fold higher concentrations than that of Fe^{3+} and the alterations in Δ*A* are all less than 5% (detection error). The results indicate that **HNABA** possesses excellent selectivity for Fe^{3+} even in the presence of other coexisting metal ions under very high concentrations.

To illustrate the response speed of **HNABA** to Fe^{3+} and the stability of the proposed system, the effect of incubation time on the absorption intensity was also investigated. The results show that a maximum and constant Δ*A* is reached after all reagents are added and incubated for *ca.* 20 min at room temperature. Δ*A* remains constant for more than 1 h, implying that the **HNABA** sensor for Fe^{3+} is stable and reliable.

The influence of ionic strength on Δ*A* of the system at 478 nm was also investigated by varying NaCl concentration from 1.0×10^{-2} mol L^{-1} to 1.0×10^{-6} mol L^{-1}. It is worth noting that all the ion strengths tested have no obvious effect on Δ*A*, hinting that the target sensing system is quite stable and may be applied in various kinds of surroundings.

Table 1 Determination results for environmental water samples ($n = 5$)[a]

Samples[b]	$C_{Fe^{3+}}$ in sample[b] (nM)	Spiked (nM)	Found (nM)	Recovery (%)	R.S.D. (%)
1 (The Pi river)	788.5	500.0	1277.7	97.8	2.2
2 (Underground)	985.2	500.0	1496.0	102.2	3.5
3 (Pure water)	0.00	500.0	492.8	98.6	1.3

[a] PB, pH 7.0. [b] The environmental water Fe^{3+} concentration determined using **HNABA** with the proposed method. The real values are the table values $\times 10^{-2}$ nmol L^{-1} for the detected water samples were concentrated 100 times.

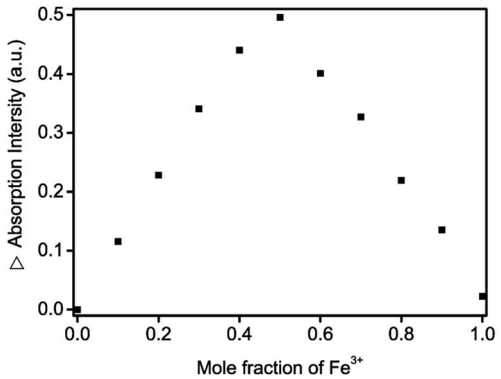

Fig. 5 Job plot of HNABA–Fe^{3+} system. [HNABA] + [Fe^{3+}] = 8.0 × 10^{-5} mol L^{-1} in aqueous at pH 7.0.

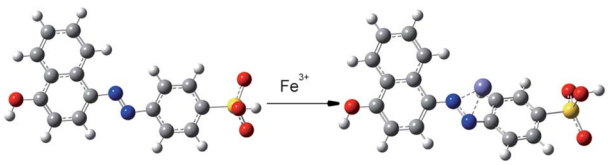

Fig. 6 Optimized geometries of HNABA before and after reaction with Fe^{3+} ion. O, N, C, H, S and Fe atom are represented as red, blue, gray, white-gray, yellow and blue-purple, respectively.

3.3 Analytical parameters and samples detection

Fig. 4 shows the colour change and the absorption spectra of **HNABA** at different concentrations of Fe^{3+} between 9.5–400 × 10^{-8} mol L^{-1}. From Fig. 4a, it is easy to find that the colour of the sensing system changes from brick-red to light red, which can be detected by the naked eye. Also, the calibration graph, the detection limit and precision for Fe^{3+} detection are obtained under the optimal conditions from Fig. 4b and c. A linear relationship between ΔA and Fe^{3+} concentration is exhibited in the range of 9.5–400 × 10^{-8} mol L^{-1} with a correlation coefficient of 0.9938. The regression equation is $A = -0.04834 \times 10^{-4} + 1.37 \times 10^{-3}c$. Based on the definition of detection limit, three times the average deviation of UV absorption at 478 nm in 20 blank samples without Fe^{3+} divided by the slope absolute value of the standard curve in Fig. 4c here, the limit of detection (LOD) for Fe^{3+} is up to 4.2 × 10^{-9} mol L^{-1}.

To confirm its feasibility, the proposed method was applied to determine Fe^{3+} in three environmental water samples from the Pi River, underground water and tap water on campus, respectively (Table 1). All the samples were obtained by filtering several times and concentrated by a factor of 100 before testing. For recovery studies, some known concentrations of Fe^{3+} were added to the environmental water samples and the total Fe^{3+} concentrations were determined following the method proposed above. The recoveries of different known amounts of Fe^{3+} spiked solution were obtained from 97.8% to 102.2% with a satisfying analytical precision (R.S.D. ≤3.5%).

3.4 Action mechanism between HNABA and Fe^{3+}

To investigate the nature of the bonding between **HNABA** and Fe^{3+}, the binding stoichiometry of **HNABA** with Fe^{3+} was determined by using a Job plot. For the Job plot analyses, a series of solutions with varying mole fractions of Fe^{3+} were prepared by maintaining the total **HNABA** and Fe^{3+} concentration constant (6.0 × 10^{-5} mol L^{-1}). The absorption intensity at 478 nm was measured for each solution. As shown in Fig. 5a 1 : 1 stoichiometry for the complex between **HNABA** and Fe^{3+} can be drawn from the Job plots,[41] which confirms that Fe^{3+} might coordinate with the nitrogen atoms in the –N=N bonds or with oxygen atoms on the naphthol rings.

Theoretical calculations have been carried out to further understand the nature of the bonding between **HNABA** and Fe^{3+}. The structures of **HNABA** before and after coordinating with Fe^{3+} are shown in Fig. 6, and were optimized using the B3LYP/6-31G level of theory and method implemented in the Gaussian 03 suite of programs.[42] From the results, we can find easily that the terminal phenyl rings were greatly distorted, because of the binding of Fe^{3+} with the nitrogen atoms in the –N=N bonds in **HNABA**, which resulted in the original conjugated system being destroyed and so the absorbance at 478 nm was reduced and even quenched.

4. Conclusions

In conclusion, a multifunctional dye, 4-(4-hydroxy-1-naphthylazo)benzenesulfonic acid (**HNABA**) possessed a strong absorption ($\varepsilon = 2.54 \times 10^4$ L mol^{-1} cm^{-1}) at *ca.* 478 nm in polar protic water and remained tremendously stable under acid or neutral conditions. Based on the results, the dye was successfully developed for trace Fe^{3+} detection with high selectivity and sensitivity under physiological pH conditions (pH 7.0). The optimal test conditions were obtained (after 20 min incubation time at room temperature under pH = 7.0, c_{HNABA} 5.0 ×

10^{-5} mol L^{-1} in water) by investigating the influences of solvent, pH, ion intensity and incubation time on detection sensitivity. The linear range for detection of Fe^{3+} in aqueous environments was 9.5–400 $\times$ 10^{-8} mol L^{-1} with a detection limit of 4.2 $\times$ 10^{-9} mol L^{-1} and a correlation coefficient of 0.9938. The mechanism of action of **HNABA** and Fe^{3+} ion was confirmed by means of Job plots, as well as experimental and theoretical deduction.

Acknowledgements

The authors gratefully acknowledge financial support from the National Natural Science Fund of China (no. 21277103) and Anhui Provincial Natural Science Fund (no. 1308085ME57).

Notes and references

1 R. K. Shervedani, A. Hatefi-Mehrjardi and A. Asadi-Farsani, *Anal. Chim. Acta*, 2007, **601**, 164–171.
2 M. Shamsipur, M. Sadeghi, A. Garau and V. Lippolis, *Anal. Chim. Acta*, 2013, **761**, 169–177.
3 J. Mao, Q. He and W. S. Liu, *Talanta*, 2010, **80**, 2093–2098.
4 P. Blatny, F. Kvasnicka and E. Kenndler, *J. Chromatogr. A*, 1997, **757**, 297–302.
5 M. J. C. Marenco, C. Fowley, B. W. Hyland, D. Galindo-Riano, S. K. Sahoo and J. F. Callan, *J. Fluoresc.*, 2012, **22**, 795–798.
6 T. A. Ali, G. G. Mohamed, M. M. I. El-Dessouky, S. M. Abou El Ella and R. T. F. Mohamed, *Int. J. Electrochem. Sci.*, 2013, **8**, 1469–1486.
7 N. R. Chereddy, S. Thennarasu and A. B. Mandal, *Dalton Trans.*, 2012, **41**, 11753–11759.
8 B. D. Wang, J. Hai, Z. C. Liu, Q. Wang, Z. Y. Yang and S. H. Sun, *Angew. Chem., Int. Ed.*, 2010, **49**, 4576–4579.
9 Y. Y. Du, M. Chen, Y. X. Zhang, F. Luo, C. Y. He, M. J. Li and X. Chen, *Talanta*, 2013, **106**, 261–265.
10 C. H. Ma, L. P. Lin, Y. Y. Du, L. B. Chen, F. Luo and X. Chen, *Anal. Methods*, 2013, **5**, 1843–1847.
11 K. G. Qu, J. S. Wang, J. S. Ren and X. G. Qu, *Chem.–Eur. J.*, 2013, **19**, 7243–7249.
12 S. H. Wang, L. Y. Du, A. M. Zhang and B. Li, *Anal. Lett.*, 1997, **30**, 2099–2107.
13 X. F. Wu, B. W. Xu, H. Tong and L. X. Wang, *Macromolecules*, 2010, **43**, 8917–8923.
14 X. S. Zhu and R. R. Jiang, *J. Fluoresc.*, 2011, **21**, 385–391.
15 M. Becuwe, P. Rouge, C. Gervais, M. Courty, A. Dassonville-Klimpt, P. Sonnet and E. Baudrin, *J. Colloid Interface Sci.*, 2012, **388**, 130–136.
16 M. M. Zareh, I. F. A. Ismail and M. H. Abd El-Aziz, *Electroanalysis*, 2010, **22**, 1369–1375.
17 B. Haghighi and A. Safavi, *Anal. Chim. Acta*, 1997, **354**, 43–50.
18 W. Ruengsitagoon, *Talanta*, 2008, **74**, 1236–1241.
19 M. Sugiyama, Y. Naraki and T. Hori, *J. Liq. Chromatogr. Relat. Technol.*, 2009, **32**, 788–800.
20 H. Matsumiya, N. Iki and S. Miyano, *Talanta*, 2004, **62**, 337–342.
21 I. A. Korobeinikova, G. B. Pronchev and A. N. Ermakov, *J. Anal. Chem.*, 2011, **66**, 740–744.
22 H. Fujii, *J. Am. Chem. Soc.*, 2002, **124**, 5936–5937.
23 S. B. Khan, M. M. Rahman, H. M. Marwani, A. M. Asiri, K. A. Alamry and M. A. Rub, *Appl. Surf. Sci.*, 2013, **282**, 46–51.
24 L. Hu, Z. Q. Yan and H. Y. Xu, *RSC Adv.*, 2013, **3**, 7667–7676.
25 L. Hu, Y. F. Zhang, L. Nie, C. G. Xie and Z. Q. Yan, *Spectrochim. Acta, Part A*, 2013, **104**, 87–91.
26 Z. Q. Yan, S. Y. Guang, H. Y. Xu and X. Y. Liu, *Analyst*, 2011, **136**, 1916–1921.
27 Z. Q. Yan, L. Hu, L. Nie and H. Lv, *Spectrochim. Acta, Part A*, 2011, **79**, 661–665.
28 E. W. Baumann, *Analyst*, 1992, **117**, 913–916.
29 M. A. Kabil and S. E. Ghazy, *Anal. Sci.*, 1995, **11**, 817–822.
30 K. J. Wallace, M. Gray, Z. L. Zhong, V. M. Lynch and E. V. Anslyn, *Dalton Trans.*, 2005, 2436–2441.
31 J. Yun and H. Choi, *Talanta*, 2000, **52**, 893–902.
32 S. Kawakubo, K. Shimada, Y. Suzuki and K. Hattori, *Anal. Sci.*, 2011, **27**, 341–344.
33 S. P. Wu, Y. P. Chen and Y. M. Sung, *Analyst*, 2011, **136**, 1887–1891.
34 B. K. Adebayo, S. Ayejuyo, H. K. Okoro and B. J. Ximba, *Afr. J. Biotechnol.*, 2011, **10**, 16051–16057.
35 S. Zareba and H. Hopkala, *J. Pharm. Biomed. Anal.*, 1996, **14**, 1351–1354.
36 A. K. Sharma and I. Singh, *Food Anal. Methods*, 2009, **2**, 221–225.
37 Z. Q. Yan, Y. F. Chen, S. Y. Guang, H. Y. Xu and L. F. Li, *Polym. Sci., Ser. B*, 2011, **53**, 535–539.
38 Z. Q. Yan, S. Y. Guang, H. Y. Xu and X. Y. Liu, *Dyes Pigm.*, 2013, **99**, 720–726.
39 Z. Q. Yan, H. Y. Xu, S. Y. Guang, X. Zhao, W. L. Fan and X. Y. Liu, *Adv. Funct. Mater.*, 2012, **22**, 345–352.
40 Z. Q. Yan, S. Y. Guang, H. Y. Xu, X. Y. Su, X. L. Ji and X. Y. Liu, *RSC Adv.*, 2013, **3**, 8021–8027.
41 H. J. Kim, J. E. Park, M. G. Choi, S. Ahn and S. K. Chang, *Dyes Pigm.*, 2010, **84**, 54–58.
42 M. J. T. Frisch, G. W. Trucks, H. B. Schlegel, G. E. Scuseria, M. A. Robb, J. R. Cheeseman, J. A. Montgomery, Jr, T. Vreven, K. N. Kudin and J. C. Burant, *Gaussian 03, revision A.1*, Gaussian, Inc., Pittsburgh, PA, 2004.

